Organo-soluble, segmented rigid-rod polyimide films: 2. Properties for microelectronic applications

Fred E. Arnold Jr, Stephen Z. D. Cheng*, Steven L.-C. Hsu, Chul Joo Lee and Frank W. Harris

Institute and Department of Polymer Science, College of Polymer Science and Polymer Engineering, The University of Akron, Akron, OH 44325-3909, USA

and Suk-Fai Lau

Research Center, Hercules, Inc., Wilmington, DE 19894, USA

(Received 14 October 1991; revised 10 February 1992; accepted 19 March 1992)

The essential properties of polyimide films of importance in microelectronic applications are thermal and thermo-oxidative stability, dimensional stability, glass transition behaviour and the relative permittivity (dielectric constant ε'). A segmented rigid-rod polyimide was synthesized from 3,3',4,4'-biphenyltetracarboxylic dianhydride (BPDA) and 2,2'-bis(trifluoromethyl)-4,4'-diaminobiphenyl (PFMB) in order to develop new materials for microelectronic applications. The thermal and thermo-oxidative stability were investigated by determining the thermal degradation activation energy in air (210 kJ mol^{-1}) and in nitrogen (303 kJ mol^{-1}). The thermal stability was further studied through thermogravimetry–mass spectroscopy. The coefficient of thermal expansion, which indicates the dimensional stability, was measured via a tension mode of a thermomechanical analyser and doubly extrapolated to zero stresses, and was $6.98 \times 10^{-6}\,°C^{-1}$ for the BPDA–PFMB films. The glass transition temperature, measured thermomechanically, was found to be 287°C. The dielectric constant for the films, measured after ageing at 50% relative humidity for 48 h at 23°C, was between 2.8 and 2.9 in a frequency range from 0.1 kHz to 1 MHz. The temperature and frequency dependence of the dielectric behaviour is also discussed.

(Keywords: coefficient of thermal expansion; dimensional stability; glass transition temperature; microelectronic application; relative permittivity; segmented rigid-rod polyimide film; thermal and thermo-oxidative stability; thermogravimetric mass spectroscopy; thermomechanical measurement)

INTRODUCTION

Aromatic polyimides exhibit excellent electrical and mechanical properties, along with high thermal and thermo-oxidative stability. These polymers also display chemical and solvent resistance, good adhesive properties and light and dimensional stability. This unique combination of properties has led to many industrial applications of polyimide products of which polyimide films are especially important.

Polyimide films are widely used as interlayer dielectrics and packaging materials. However, these aromatic polyimides are difficult, if not impossible, to process thermotropically since they often possess a transition temperature which is close or even above the decomposition temperature. In fact, aromatic polyimides are usually processed in their poly(amic acid) precursors, and then either thermally or chemically imidized. An example of this procedure is poly(4,4'-oxydiphenylene-pyromellitimide) (PMDA–ODA), which is commercially produced by Dupont under the trade name of Kapton®[1–3].

Recently, a family of organo-soluble rigid-rod and segmented rigid-rod aromatic polyimides has been synthesized in our laboratory[4]. The polymer was synthesized from 3,3',4,4'-biphenyltetracarboxylic dianhydride (BPDA) and 2,2'-bis(trifluoromethyl)-4,4'-diaminobiphenyl (PFMB) in refluxing *m*-cresol in a one-step process. The intermediate poly(amic acids) were not isolated. The chemical structure of BPDA–PFMB is

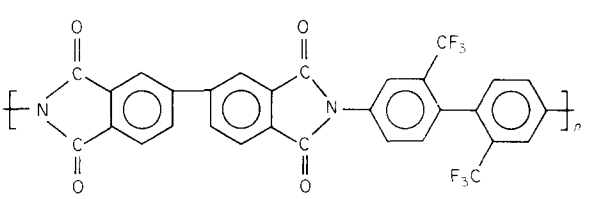

with a repeating unit of 578.5 g mol^{-1}. The first paper of this series concerned the structure formation in unoriented BPDA–PFMB films[5]. This was monitored during the annealing process through the reflection and transmission modes of wide angle X-ray diffraction (WAXD) experiments. It was found that the *c*-axis of the crystals undergoes an orientation process which results in it being parallel to the film surface (an in-plane

*To whom correspondence should be addressed

0032-3861/92/245179-07
© 1992 Butterworth-Heinemann Ltd.

orientation). It was predicted that based on the chain rigidity, the chain molecules may also possess an in-plane orientation[5]. This kind of anisotropy has been found previously in other polyimide thin films[6–11].

In this paper we focus on several properties of BPDA–PFMB films that are important for microelectronic applications. One needs a high thermal and thermo-oxidative stability which may be expressed through either the temperature at which a 5% weight loss of the polymer occurs (in air and/or nitrogen)[12] or, more quantitatively, the determination of a thermal degradation activation energy measured by thermogravimetry (t.g.). Furthermore, the stability of the pendant groups as well as the polymer backbone, observed through a t.g. coupled with mass spectroscopy (m.s.), will give the detailed degradation mechanism which is important in determining use conditions. The coefficient of thermal expansion (CTE) of the polymer measured through thermomechanical analysis (t.m.a.) must be of the same order of magnitude compared with common substrates such as copper, silicon or silicon dioxide. A mismatch between the CTE of the film and that of the particular substrate could be detrimental to long-term use. Moreover, the CTE should be retained at high temperatures, namely, a high glass transition temperature is necessary. On the other hand, the relative permittivity (dielectric constant ε') must be as low as possible in order to minimize the RC time constant which represents the access times to the individual memory cell. Note that poly(tetrafluoroethylene) (PTFE) possesses a dielectric constant of 2, which is the lowest value measured in polymers. The Kapton® polyimide (PMDA–ODA) film shows a dielectric constant of about 3.2–3.5, depending upon measurement conditions, which is common among unfluoronated polyimides. From our experimental observations, BPDA–PFMB film exhibits excellent properties which meet the requirements described above, and may serve as a potential candidate as an interlayer dielectric for applications in multilevel very large scale integrated circuits.

EXPERIMENTAL

Materials and sample preparation

The polymer was synthesized from BPDA and PFMB. The detailed procedure has been published elsewhere[4]. Concentration of the polymer after polymerization is 8–10% (w/w). The polymer remains completely in solution when the temperature is above 140°C. During cooling, the polymer undergoes a sol–gel transition and upon standing, ordered structures develop in the gel state[13,14]. The intrinsic viscosity of BPDA–PFMB in *m*-cresol at 60°C is 4.5 dl g^{-1}.

BPDA–PFMB powders were prepared through precipitation of the BPDA–PFMB solution in ethanol. The powders were heated at 280°C in a vacuum oven for 5 h in order to evaporate any residual solvent before the thermal degradation study. On the other hand, BPDA–PFMB films were cast through a 2% (w/w) solution on a glass plate with a doctor's knife, followed by drying at 150°C for 5 h under reduced pressure in a vacuum oven, and further heated to 300°C for 5 min on a thermomechanical analyser in dry nitrogen. During the heat treatment, the film was heated with its edges fixed and under a predetermined tensile stress (0.5, 1.0 or 2.0 MPa). The thickness of the films ranged from 20 to 30 μm. Precise control of the concentration and the thickness of the casting dope on the glass plate were necessary to control the final thickness of the films.

Experiments and equipment

Thermal degradation experiments in air and dry nitrogen were conducted on a Seiko TG/DTA 200 system. An isothermal mode was adopted in order to obtain degradation activation energies of the polymer. The temperature range is 400–530°C. The weight loss with respect to time was recorded at different isothermal temperatures. A typical sample weight of 3 mg was used.

Polymer backbone and pendant group degradation was studied using t.g.–m.s. Detailed instrument set-up is described in ref. 15. An initial sample weight of 4.9 mg was used with a temperature range of approximately 30–900°C in vacuum.

A thermomechanical analyser (TA TMA 2940) was used to determine the glass transition temperature (T_g) and the linear CTE for the BPDA–PFMB thin films. Due to the thickness of the films, it was decided to use the tension mode at different applied stresses, ranging from 1 to 10 MPa. Ribbon-shaped film samples with an average cross-sectional area of 0.09 mm^2 were cut and heat-treated at 300°C for 5 min at different initial tensile stresses. A heating rate of 15°C min^{-1} was used with a temperature range of 30–450°C. The CTEs were calculated from the slopes of the experimental plots between the percentage of elongation and temperature in a temperature range of 50–200°C. When the temperature approached the glass transition temperature, a dramatic increase in the CTE was observed. The onset temperature of this change is recognized as the glass transition temperature obtained under a particular applied stress.

Dielectric measurements were carried out in two different experiments. The first experiment was to determine the relative permittivity using the procedure described in ASTM D-150-81. The film samples were gold-coated on both sides via vacuum evaporation deposition and then aged at 23°C under 50% relative humidity for 48 h. They were measured at 23°C using a capacitance bridge (General Radio-716C) at four different frequencies (1 kHz, 10 kHz, 100 kHz and 1 MHz). The second experiment was to observe the temperature dependence of the dielectric behaviour. A TA 2100/DEA 2970 system was used on the same gold-coated samples from the previous experiment (ASTM D-150-81). The measurements were performed in a frequency range of 0.1–100 kHz with a heating rate of 2°C min^{-1} under a dry nitrogen atmosphere. The maximum force applied on the sample was 500 N, while the minimum sample thickness was controlled at 20–25 μm. The calculation of dielectric constants was based on the film thickness at room temperature.

RESULTS AND DISCUSSION

Thermal degradation activation energies and mechanism

Thermal degradation kinetics were carried out under isothermal conditions. *Figures 1* and *2* show isothermal changes in percentage weight loss with time at different temperatures (400–530°C) in a dry nitrogen atmosphere and in air, respectively. It is clear from *Figure 1*, for example, that over 5 h at 460°C only about 1% weight loss is observed. At 510°C about 90% of the weight is

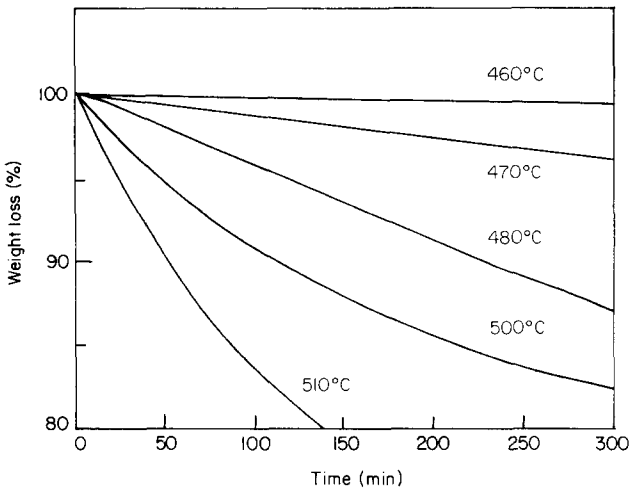

Figure 1 Isothermal degradation relationships between the percentage weight loss changes and time for BPDA–PFMB at different temperatures in nitrogen

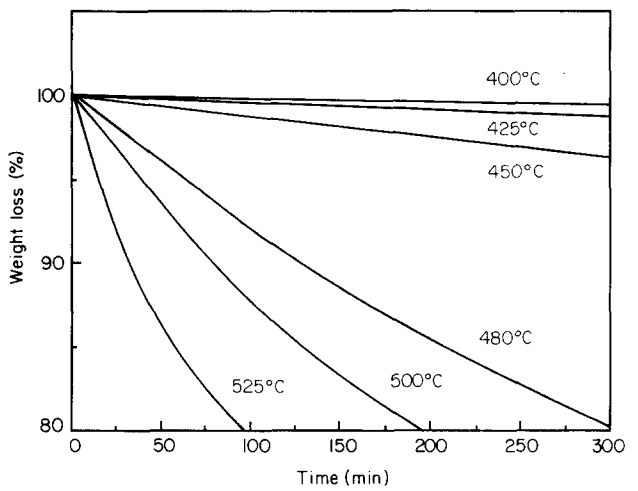

Figure 2 Isothermal degradation relationships between the percentage weight loss changes and time for BPDA–PFMB at different temperatures in air

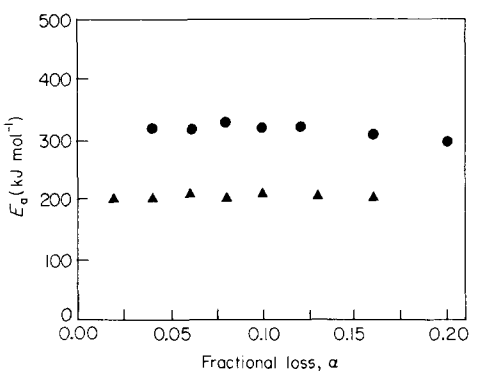

Figure 3 Relationships between the thermal degradation activation energy (E_a) and conversion (α), calculated from equation (1): ●, in nitrogen; ▲, in air

retained after 1 h of the experiment. On the other hand, the isothermal change in weight loss is about 1% at 400°C in air (*Figure 2*), which is 60°C lower than the same weight loss in dry nitrogen. Based on an integrated rate expression suggested by Flynn[16] (see also ref. 17) one can follow the equation:

$$\ln t = \ln g(\alpha) - \ln A + E_a/RT \qquad (1)$$

where t is the isothermal time, $g(\alpha)$ is the integration of the rate of weight loss, A is the pre-exponential factor, R is the universal gas constant and E_a is the thermal degradation activation energy. The slope of a plot between $\ln t$ and $1/T$ at constant fractional loss (α), yields the activation energy, as shown in *Figure 3*. The calculated E_a (under nitrogen) ranges from 320 kJ mol^{-1} at $\alpha = 4.0\%$ to 291 kJ mol^{-1} at $\alpha = 20\%$ conversion. The average value of the activation energy is 303 kJ mol^{-1} in dry nitrogen. Also shown in *Figure 3* is the degradation activation energy determined in air, in which an average value of 210 kJ mol^{-1} was observed.

In order to learn about the detailed thermal degradation mechanism, t.g.–m.s. was carried out at a heating rate of 3°C min^{-1}. The temperature dependence of the total ionization current is shown in *Figures 4* and *5*. The maximum arises from the release of six major products: these are CO, HCN, NH_3, HF, COF_2 and CF_3H arising from thermal cracking of the diimide and pendant loss. The overall profile indicates that a maximum rate of thermal degradation (vacuum condition) occurs at around 595°C. The results illustrate that the degradation of the pendant groups has a maximum intensity of around 580°C as indicated by the CF_3H ion (*Figure 4*). The thermal stability of the pendant trifluoromethyl groups is of paramount importance. A low dielectric constant is vital for microelectronic use. The electron withdrawing nature of the pendant trifluoromethyl groups is responsible for lowering the dielectric constant in films by their conformational arrangements of dipole cancellation. At higher temperatures, as indicated in *Figure 5*, we observe the main chain degradation products through the HCN and NH_3 ions.

Coefficient of thermal expansion

Figure 6 shows the solid state CTE (between 50 and 200°C) measured at different applied stresses. The film was previously heat-treated at 300°C for 5 min under an initial tensile stress of 0.5 MPa. As the magnitude of the

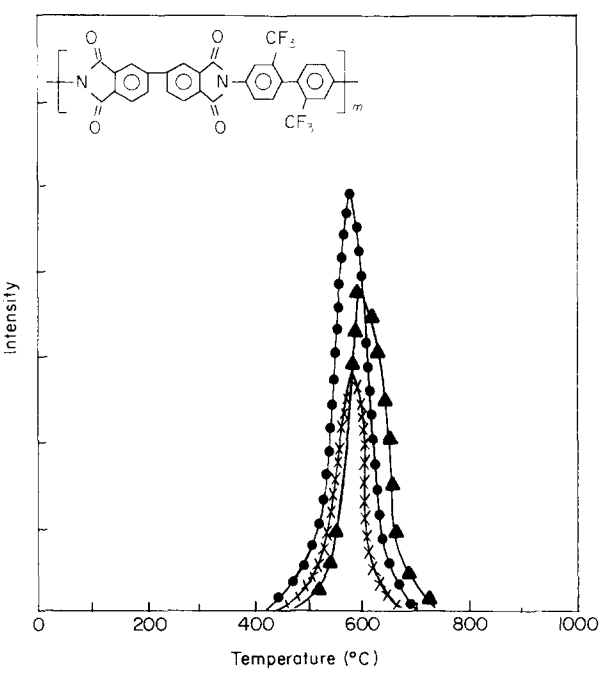

Figure 4 T.g.–m.s. results for the pendant group degradation under vacuum: ●, CF_3H; ×, COF_2 (×20); ▲, HF

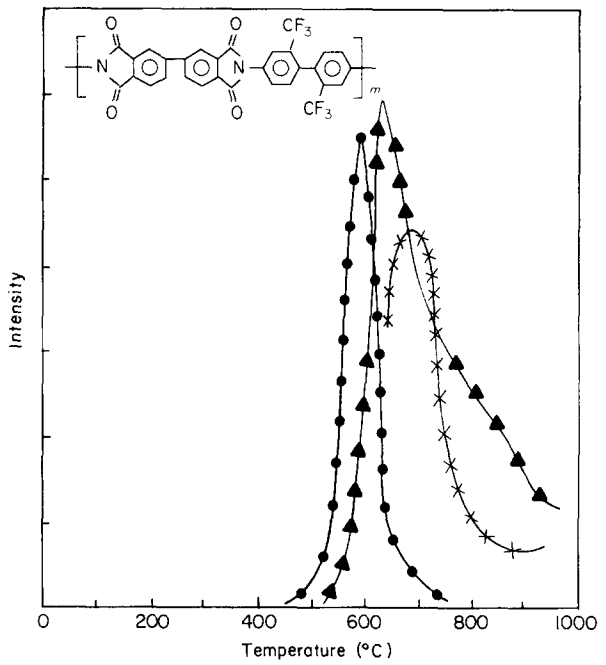

Figure 5 T.g.–m.s. results for the main backbone chain degradation under vacuum: ●, CO; ▲, HCN; ×, NH_3

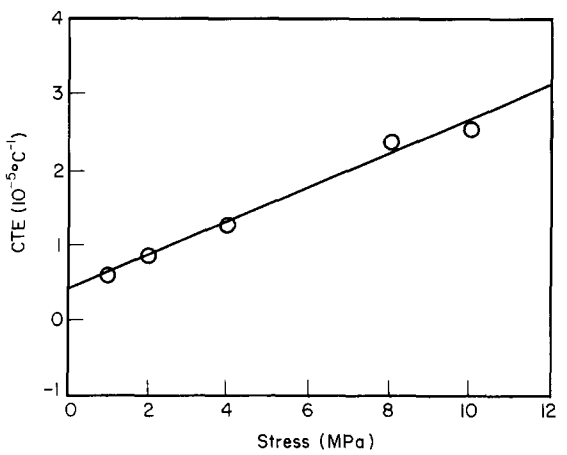

Figure 6 Relationship between CTE in the temperature range 50–200°C and applied stress for BPDA–PFMB films under an initial tensile stress of 0.5 MPa during heat treatment

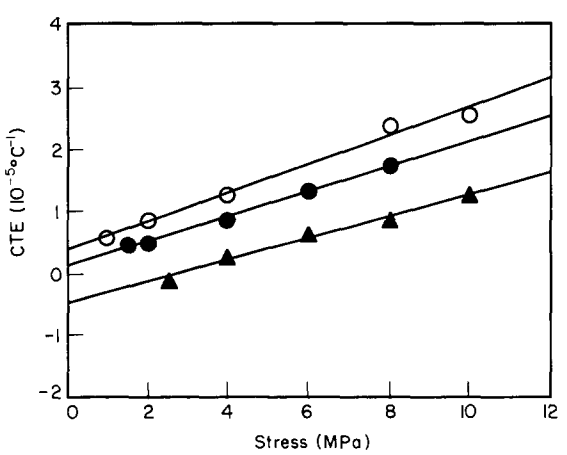

Figure 7 Relationship between CTE in the temperature range 50–200°C and applied stress under three different initial tensile stresses: ○, 0.5 MPa; ●, 1.0 MPa; ▲, 2.0 MPa

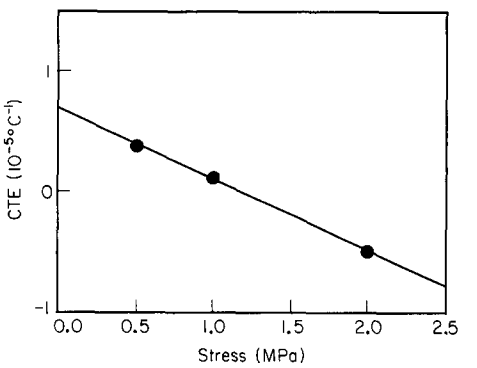

Figure 8 Extrapolation of CTE to zero initial tensile stress to obtain the true CTE for BPDA–PFMB films

applied stress is increased, the CTE in the glassy state increases linearly in a stress region of 1–10 MPa. Since the CTE is dependent on the initial tensile stress during the heat treatment and the applied stress during the measurements, we must extrapolate both stresses to zero (double extrapolation). This is necessary for the unoriented BPDA–PFMB film in order to obtain its true CTE. The first extrapolated value is $3.89 \times 10^{-6}\,°C^{-1}$ for the BPDA–PFMB film, which was under an initial tensile stress of 0.5 MPa. *Figure 7* shows the effect of the CTE in changing the initial tensile stress during the heat treatment (second extrapolation). A stress dependency can be observed in the CTE data. For example, an extrapolated value of $1.22 \times 10^{-6}\,°C^{-1}$ is observed using an initial tensile stress of 1.0 MPa during the heat treatment. Upon increasing this stress (from 0.5 to 2.0 MPa) during the initial heat treatment, the extrapolated CTE changes from 3.89×10^{-6} to $-4.9 \times 10^{-6}\,°C^{-1}$. Apparently, with increasing the initial tensile stress, a decrease in the extrapolated CTE is evident. Extrapolating this initial tensile stress to zero (*Figure 8*) yields a CTE of $6.98 \times 10^{-6}\,°C^{-1}$. The CTE measured from the samples that were heat-treated at 2.0 MPa exhibits a negative CTE after extrapolation to zero stress. This indicates that during the heat treatment some additional anisotropy is introduced into the sample, resulting in partial orientation in the films. It should be understood that a molecular explanation of thermal expansion behaviour in the solid state is due to an unharmonic potential interaction between atoms and/or molecules. A negative CTE may only be attributed to a change of molecular packing and/or stress relaxation. It is also noted that the CTE of copper is $16.6 \times 10^{-6}\,°C^{-1}$, and that of silicon is $3 \times 10^{-6}\,°C^{-1}$. Thus the CTE of BPDA–PFMB films is in between the values of copper and silicon, which are two important inorganic materials widely used for microelectronic applications.

Several years ago, a series of CTE data for some aromatic polyimides was reported[18–22]. Most of the polymers had CTEs ranging from 10×10^{-6} to $70 \times 10^{-6}\,°C^{-1}$. It was found that the polyimides obtained from BPDA or PMDA, and diamines which were composed of only phenylene groups fused at the *para* position, possessed CTEs below $10 \times 10^{-6}\,°C^{-1}$. The closest polyimides to BPDA–PFMB were polymers made from BPDA synthesized with *p*-phenylene diamine, *o*-tolidine and 4,4′-diaminoterphenyl; their respective CTEs were 19×10^{-6}, 9.2×10^{-6} and $14 \times 10^{-6}\,°C^{-1}$ in the case of free cure condition, and 2.6×10^{-6},

5.4×10^{-6} and $5.9 \times 10^{-6}\,°C^{-1}$ in the case of bifixed cure condition[19,22]. Since these polyimides were converted from their poly(amic acid) precursors, the cure condition, which governs the film's morphology and properties, is important[6–10,23]. Nevertheless, our results are still close to the literature data in the case of bifixed cure condition. On the other hand, the CTE of Kapton® film is $47 \times 10^{-6}\,°C^{-1}$ for the free cure condition and $27 \times 10^{-6}\,°C^{-1}$ for the bifixed cure condition[22]. Another example is polybenzobisthiazole (PBZT), for which the CTE is $7 \times 10^{-6}\,°C^{-1}$ or less in the direction parallel to the film surface[24]. It should be noted that the CTEs of linear flexible polymers are about one order of magnitude higher than that of BPDA–PFMB films. For example, the CTE of polyethylene is $\sim 95 \times 10^{-6}\,°C^{-1}$, while that of PTFE is $\sim 99 \times 10^{-6}\,°C^{-1}$.

A general understanding of the low CTE is the result of chain rigidity, linear chain conformation and intermolecular cohesive energy. However, the attempt to establish a quantitative relationship between chemical structure, molecular packing and CTE was not successful[20]. It was found that crystallinity in polyimide films does not correlate to the CTE of the films. On the other hand, the linearity of chain conformation seems to play an important role[22]. We speculate that the CTE may be affected not only by the linearity of chain conformation, but also by the orientation of the molecules. The degree of in-plane orientation could significantly affect the thermal expansion behaviour of the thin film. Chain rigidity and linear chain conformation are necessary conditions for such an in-plane orientation. The crystallinity effect could not be detected since the density difference between the crystal and the amorphous state for BPDA–PFMB is rather small compared to most polymers[1,2].

Another important material parameter is the glass transition temperature, T_g, of BPDA–PFMB films. Using the onset temperature of the CTE change as T_g, it is evident that T_g decreases linearly with increasing applied stress in the t.m.a. measurements, as shown in *Figure 9*. The linear extrapolation yields a T_g without an applied stress ($\sigma = 0$, T_g°) of 287°C and a slope of 6.58°C min^{-1}. The slope indicates how sensitive T_g is with respect to the applied stress. It is evident from *Figure 9* that different initial tensile stresses during heat treatment do not significantly affect T_g. Similar experimental observations between T_g and σ were reported for poly(methyl methacrylate) (PMMA)[25], polyvinyl chloride (PVC)[26–28] and polycarbonate (PC)[29] in a relatively narrow and small stress range. In fact, the linear relationship deviates at higher applied stresses such as in the case of highly oriented BPDA–PFMB single filaments[30].

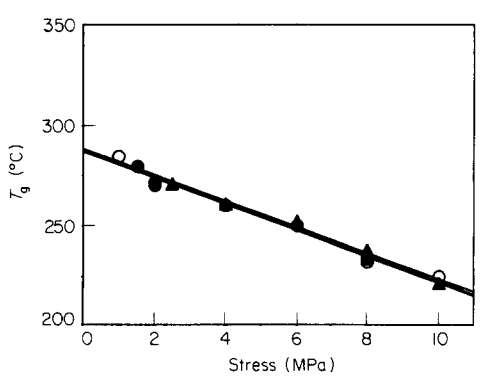

Figure 9 Dependence of glass transition temperature (T_g) on applied stress from t.m.a. The extrapolated T_g is 287°C at $\sigma = 0$ under three different initial tensile stresses: ○, 0.5 MPa; ●, 1.0 MPa; ▲, 2.0 MPa

The microscopic explanation of the decrease in T_g with increasing σ was earlier qualitatively suggested to be caused by an increase in free volume with an applied stress[31]. Quantitative treatment was not possible until Chow[32,33] proposed a theoretical prediction of yield stress *versus* T_g based on his multiple-hole energy model[34], the kinetics of glass transition[25,26], volume relaxation, memory behaviour[35] and the equation of state for polymeric liquids and glasses[36]. When a system is under a uniform tensile stress (σ) with negligible strain rate, the effect of an applied stress on T_g can be described by[32,33]:

$$T_g = T_g^\circ + \frac{RT_r^2}{\bar{\varepsilon}}\left[1 - \exp\left(\frac{\sigma V}{RT_g^\circ}\right)\right] \qquad (2)$$

where $\bar{\varepsilon}$ is the average energy of hole formation, T_r is a reference temperature, V is the tensile-activation volume and R is the universal gas constant. If $\sigma = 0$, equation (2) reduces to $T_g = T_g^\circ$, and if σ is small and approaches zero, equation (2) becomes[32,33]:

$$T_g \simeq T_g^\circ - \frac{T_r \sigma V}{\bar{\varepsilon}} = T_g^\circ - K\sigma \qquad (3)$$

where $K = T_r V/\bar{\varepsilon}$ (°C MPa^{-1}). The detailed derivation requires that the exponential term in equation (2) can be expanded in a series when $\sigma V \ll 1$. Equation (3) gives rise to a molecular explanation of this linear relationship between T_g and σ, which was proposed earlier by Haward based on experimental observations[37]. For BPDA–PFMB films under a heating rate of 15°C min^{-1}, equation (3) represents the experimental results as illustrated in *Figure 9* in a stress range below 10 MPa.

Further discussion can be made based on the data of CTEs in the solid and liquid states as well as T_g°. Empirically, Simha and Boyer[38] suggested that the volumetric CTEs obey the equation:

$$[\mathrm{CTE}_{\mathrm{liquid}} - \mathrm{CTE}_{\mathrm{solid}}]\,T_g^\circ \approx 0.115 \qquad (4)$$

For the linear CTEs, the constant in equation (4) should thus be reduced to 0.0383 since a linear CTE is one-third of its volumetric CTE in an isotropic bulk sample. Based on this equation, the linear CTE data of BPDA–PFMB in both the solid and liquid states yields a value of 0.025 if a T_g value of 287°C is used. This value is slightly lower than the universal value of 0.0383. The deviation may be caused by the anisotropic nature of the films (in-plane orientation).

Dielectric properties

Under the test conditions of ASTM D-150-81, namely, ageing at 50% relative humidity for 48 h at 23°C and measured at four different frequencies (1 kHz, 10 kHz, 100 kHz and 1 MHz), BPDA–PFMB films show relative permittivities (ε') of 2.89, 2.87, 2.85 and 2.84, respectively. These values are considerably lower than that of PMDA–ODA[39] ($\varepsilon' = 3.5$ at 1 kHz and 3.3 at 10 MHz). Dielectric constants for various rigid-rod and segmented rigid-rod polyimides have also been reported[40,41] ranging from 2.39 to 3.22. It was observed that with increasing fluorine content within the polymer the dielectric constant decreases[40,42,43]. The ε' data are

lower than those of most thermoplastics such as copolyesters[44,45], polyamides[46] and epoxy resins[47]. The dielectric constant of BPDA–PFMB is comparable to many linear flexible macromolecules, as shown in *Table 1*. The importance of a low dielectric constant in thin films can be recognized from a decrease in the resistor/capacitor (RC) effect when the film is used as an insulator in computer chips, resulting in an increase in computation speed.

The dielectric properties are temperature and frequency dependent, which is an essential feature in microelectronic applications. *Figures 10* and *11* show, respectively, the dielectric constant and tan δ (dissipation factor) dependence on temperature at four different frequencies (0.1, 1.0, 10, 100 kHz). It is interesting to note from *Figure 10* that the dielectric constant remains almost constant until about 210°C. A gradual increase of ε' can be observed with further increasing temperature until a

Table 1 Dielectric constants (ASTM D-150)

Materials	Low value (ε')
Poly(tetrafluoroethylene)	2.0
Poly(proplene)	2.2
Poly(ethylene), medium density	2.25
Poly(styrene), general purpose	2.45
BPDA–PFMB	2.8–2.9
PMDA–ODA (Kapton®)	3.2–3.5

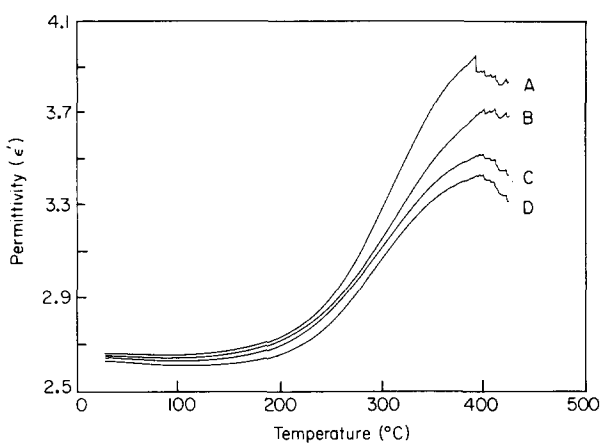

Figure 10 Dielectric constant (ε') changes with temperature at four different frequencies: A, 0.1 kHz; B, 1 kHz; C, 10 kHz; D, 100 kHz

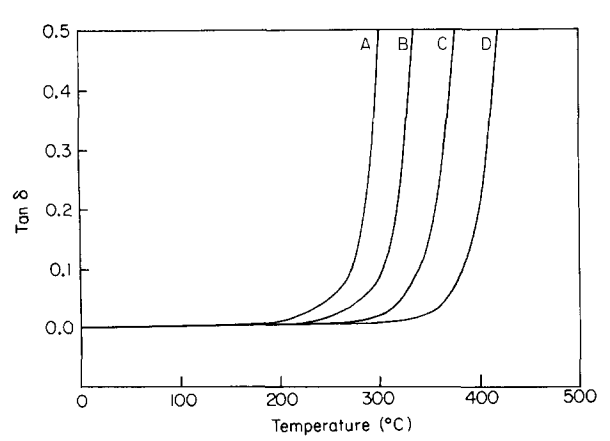

Figure 11 Dissipation factor (tan δ) changes with temperature at four different frequencies: A, 0.1 kHz; B, 1 kHz; C, 10 kHz; D, 100 kHz

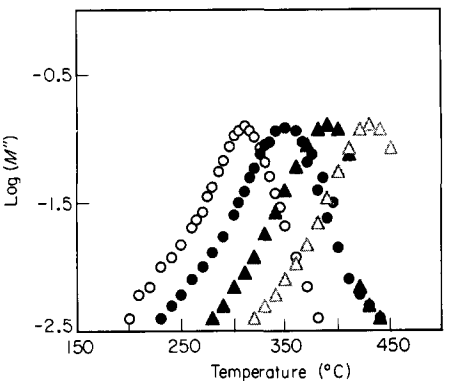

Figure 12 Relationship between electric loss modulus (log M'') and temperature at four different frequencies: ○, 0.1 kHz; ●, 1.0 kHz; ▲, 10 kHz; △, 100 kHz

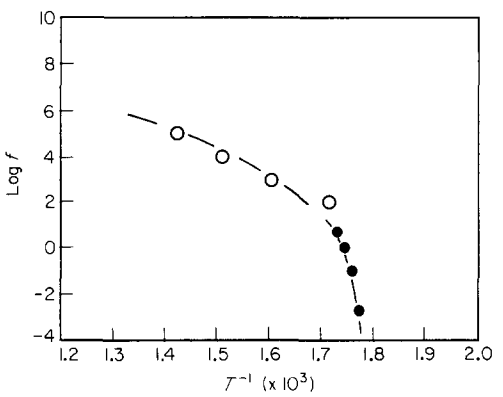

Figure 13 Relationship between logarithmic frequency and reciprocal loss peak temperatures: ○, data from DEA; ●, data from d.m.a.[49]

frequency dependent maximum is reached at about 290°C. On the other hand, the dissipation factor (tan δ) exhibits a frequency dependence with a sharp increase occurring at higher temperatures, corresponding to the higher frequencies. This rapid increase with no observable maxima in *Figure 11* is caused by ion conduction which only contributes to the loss factor (ε''). One can use the concept of electric loss modulus, M'', which is defined as $\varepsilon''/(\varepsilon'^2 + \varepsilon''^2)$, to illustrate the relaxation process[48]. A plot of logarithmic M'' *versus* temperature is shown in *Figure 12* for BPDA–PFMB films. A well defined peak at each frequency is identified. To further identify the nature of this relaxation process, a relationship between logarithmic frequency and reciprocal peak temperature is plotted in *Figure 13*, which also includes dynamic mechanical data (loss modulus peaks) at low frequencies[49]. A non-linear relationship is obtained over the wide frequency range rather than a straight line which illustrates a single activation energy. This behaviour of the dielectric relaxation is similar to that of viscosity and can be treated by a Williams–Landel–Ferry (WLF)-type equation:

$$\log(f) = \frac{a(T - T_o)}{b + (T - T_o)} \qquad (5)$$

The relaxation data could be fitted to equation (5) using a reference temperature of 295°C at 0.002 Hz. One can thus conclude that the dielectric relaxation process must be the result of the glass transition of the material.

Up to now, we have only studied the CTE parallel to the film surface and the dielectric properties perpendicular

to the film surface. Since BPDA–PFMB films possess an 'in-plane orientation', one expects anisotropic behaviour when investigating thermal expansion and dielectric behaviour. The anisotropic properties will be investigated in a future publication.

CONCLUSION

In studying the properties of a segmented rigid-rod polyimide film (BPDA–PFMB), it has been observed that:

(1) the films exhibit a high thermal and thermo-oxidative stability with a degradation activation energy of 210 kJ mol^{-1} in air and 303 kJ mol^{-1} in dry nitrogen;
(2) a high dimensional stability is observed with a CTE of 6.98×10^{-6} $°C^{-1}$ in a temperature region of 50–200°C;
(3) a low dielectric constant of around 2.8–2.9 at room temperature which is dielectrically stable up to 210°C in a frequency range above 0.1 kHz;
(4) a glass transition temperature of 287°C measured through t.m.a. and supported by dielectric analysis (DEA) and d.m.a.

With the combination of the properties mentioned above, BPDA–PFMB film should be considered as a potential candidate for microelectronic applications.

ACKNOWLEDGEMENTS

This research was supported by the Material Research Division of the National Science Foundation (DMR-8920147) through the Science and Technology Center of Advanced Liquid Crystal Optical Materials (ALCOM) at Kent State University, The University of Akron and Case Western Reserve University. The synthesis of BPDA–PFMB was supported by a NASA-Langley Research Center Grant (NAG-1-448). S.Z.D.C. gratefully acknowledges the support of a Presidential Young Investigator Award (DMR-9157738) from the National Science Foundation. The authors thank Dr E. Grant Jones of Systems Research Laboratories, Inc., Dayton, Ohio for performing the t.g.–m.s. spectroscopic measurements.

REFERENCES

1 Sroog, C. E. *J. Polym. Sci.* 1967, **16**, 1191
2 Sroog, C. E. *J. Polym. Sci. Macromol. Rev.* 1976, **11**, 161
3 Lee, H., Stoffey, D. and Neville, K. 'New Linear Polymers', McGraw Hill, New York, 1967, pp. 183, 224
4 Harris, F. W. and Hsu, S. L. C. *High Perform. Polym.* 1989, **1**, 1
5 Cheng, S. Z. D., Arnold, F. E., Zhang, A.-Q., Hsu, S. L.-C. and Harris, F. W. *Macromolecules* 1991, **24**, 5856
6 Ikeda, R. M. *J. Polym. Sci., Polym. Lett. Edn* 1966, **4**, 353
7 Russell, T. P., Gugger, H. and Swalen, J. D. *J. Polym. Sci., Polym. Phys. Edn* 1983, **21**, 1745
8 Isoda, S., Shimada, H., Kochi, M. and Kambe, H. *J. Polym. Sci., Polym. Phys. Edn* 1981, **19**, 1293
9 Russell, T. P. *J. Polym. Sci., Polym. Phys. Edn* 1984, **22**, 1105
10 Takahashi, N., Yoon, D. Y. and Parrish, W. *Macromolecules* 1984, **17**, 2583
11 Yoon, D. Y., Ree, M., Volhsen, W., Depero, L. and Parrish, W. in 'Materials Science of High Temperature Polymers for Micro-Electronics', Vol. 227, MRS Symposium Proceedings, Pittsburgh, PA, 1991
12 Cheng, S. Z. D., Wu, Z.-Q., Eashoo, M., Hsu, S. L.-C. and Harris, F. W. *Polymer* 1991, **32**, 1803
13 Cheng, S. Z. D., Lee, S. K., Kyu, T., Hsu, S. L.-C., Lee, J. C. and Harris, F. W. *Polym. Int.* in press
14 Cheng, S. Z. D., Lee, S. K., Barley, J. S., Hsu, S. L.-C. and Harris, F. W. *Macromolecules* 1991, **24**, 1883
15 Jones, E. G., Pedrick, D. L. and Goldfarb, I. J. 44th Annual Technical Conference of SPE, Brookfield, CT, 1986, p. 434
16 Flynn, J. H. in 'Laboratory Preparation for Macromolecular Chemistry' (Ed. E. McCuffrey), McGraw Hill, New York, 1970, p. 255
17 Dickens, B. and Flynn, J. H. *Adv. Chem. J.* 1983, **203**, 209
18 Numata, S., Oohara, S., Imaizumi, J. and Kinjo, N. *Polym. J. (Jpn)* 1985, **17**, 981
19 Numata, S., Oohara, S., Fajisaki, K., Imaizumi, J. and Kinjo, N. *J. Appl. Polym. Sci.* 1986, **31**, 101
20 Numata, S., Fujisaki, K. and Kinjo, N. *Polymer* 1987, **28**, 2282
21 Numata, S. and Kinjo, N. *Polym. Eng. Sci.* 1988, **28**, 906
22 Numata, S. and Miwa, T. *Polymer* 1989, **30**, 1170
23 Wachsman, E. D. and Frank, C. W. *Polymer* 1988, **29**, 1191
24 Lusignea, R. W. in 'The Materials Science and Engineering of Rigid-Rod Polymers' (Eds W. W. Adams, R. K. Eby and D. E. McLemore), Vol. 134, MRS Symposium Proceedings, Pittsburgh, PA, 1985, p. 265
25 Huntsberger, J. R. *Polym. Eng. Sci.* 1974, **14**, 702
26 Shen, M. C. and Eisenberg, A. *Progr. Solid State Chem.* 1966, **3**, 407
27 Andrews, R. D. and Kazame, Y. *J. Appl. Phys.* 1967, **38**, 4118
28 Rawson, F. F. and Rider, J. G. *J. Polym. Sci. C* 1971, **33**, 87
29 Banwens-Crowet, C., Banwens, J.-C. and Homes, G. *J. Mater. Sci.* 1972, **7**, 176
30 Eashoo, M., Cheng, S. Z. D., Wu, Z.-Q., Shen, D.-X., Hsu, S. L.-C. and Harris, F. W. in preparation
31 Ward, I. M. in 'Mechanical Properties of Solid Polymers', Wiley, New York, 1971, Ch. 11
32 Chow, T. S. *Polym. Eng. Sci.* 1984, **24**, 915, 1079
33 Chow, T. S. *J. Polym. Sci., Polym. Phys. Edn* 1987, **25**, 137
34 Chow, T. S. *J. Chem. Phys.* 1983, **79**, 4602
35 Chow, T. S. *Macromolecules* 1984, **17**, 2336
36 Chow, T. S. *J. Rheol.* 1986, **30**, 729
37 Haward, R. N. in 'Physics of Glassy Polymers', Wiley, New York, 1973, p. 357
38 Simha, R. and Boyer, R. F. *J. Chem. Phys.* 1962, **37**, 1003
39 'Kapton® Polyimide Film – Summary of Properties', Industrial Films Division, Polymer Products Department, Dupont Company, Wilmington, DE, 1989
40 St Clair, A. K., St Clair, T. L. and Winfree, W. P. *Proc. ACS PMSE* 1988, **59**, 28
41 Stoakley, D. M. and St Clair, A. K. *Proc. ACS PMSE* 1988, **59**, 33
42 Matsura, T., Nishi, S., Ishizana, M., Yamada, Y. and Hasuda, Y. *Pacific Polym. Prepr.* 1989, **1**, 87
43 Matsura, T., Nishi, S., Ishizana, M., Yamada, Y. and Hasuda, Y. *Macromolecules* 1991, **24**, 5001
44 Kalika, D. S. and Yoon, D. Y. *Macromolecules* 1991, **24**, 3404
45 Kalika, D. S. Yoon, D. Y., Jannell, P. and Parrish, W. *Macromolecules* 1991, **24**, 3413
46 Weast, R. C. and Astle, M. J. (Eds) 'CRC Handbook of Chemistry and Physics', CRC Press, Boca Raton, 1982, p. E56
47 Lynch, C. T. 'CRC Handbook of Material Science, Vol. 3, Nonmetallic Materials and Application', CRC Press, Cleveland, 1975, p. 22
48 Starkweather, H. W. Jr and Avakian, P. *J. Polym. Sci., Polym. Phys. Edn* 1992, **30**, 637
49 Arnold, F. E. Jr, Shen, D.-X., Lee, C. J., Harris, F. W. and Cheng, S. Z. D. *J. Mater. Chem.* submitted